

An application of renormalization in Hilbert space at phase transition points in strongly interacting systems

Tarek Khalil *

and

Jean Richert †

Laboratoire de Physique Théorique, UMR 7085 CNRS/ULP,
Université Louis Pasteur, 67084 Strasbourg Cedex,
France

April 1, 2022

Abstract

We introduce an algorithm aimed to reduce the dimensions of Hilbert space. It is used here in order to study the behaviour of low energy states of strongly interacting quantum many-body systems at first order transitions and avoided crossings. The method is tested on different frustrated quantum spin ladders with two legs. The role and importance of symmetries are investigated by using different bases of states.

PACS numbers: 03.65.-w, 64.60.Ak, 64.60.Fr, 71.10.Hf

1 Introduction.

The investigation of the spectral properties of strongly interacting microscopic many-body quantum systems necessitates the use of non-perturbative

*E-mail address: khalil@lpt1.u-strasbg.fr

†E-mail address: richert@lpt1.u-strasbg.fr

approaches. Most of these rest on the renormalization group concept introduced by Wilson [1] and universally used since in all fields of quantum physics. This is the case for the study of lattice quantum systems for which the Real Space Renormalization Group (RSRG) [2, 3, 4] and the Density Matrix Renormalization Group (DMRG) [5, 6, 7] have been introduced in order to reduce the dimensions of the systems. More generally the particular property of the renormalization methods is the fact that they can reveal the existence and location of phase transitions which are characterized as fixed points, i.e. the coupling strengths which define the Hamiltonian or the action of the systems and evolve during the renormalization process (running coupling constants) stay constant at these specific points, both in the case of discontinuous and continuous transitions [7, 8].

The reduction process has mainly been applied in d -dimensional real and momentum space. In the present approach we introduce a reduction algorithm which operates in $0d$ Hilbert space. The spectral properties of quantum systems are obtained through the diagonalization of a many-body Hamiltonian acting in a complete, in general infinite or at least very large set of basis states although the information of interest is restricted to the knowledge of a few low-energy states.

In order to avoid the diagonalization of very large matrices we recently proposed a non-perturbative approach which tackles this question [9]. We implemented it in the study of strongly interacting systems like frustrated two-leg ladders [10]. The approach consists of a step by step reduction of the size of Hilbert space by means of a projection technique. It induces a renormalization process in the spirit of former work [11, 12, 13]. Its advantage over other reduction procedures lies in the fact that it is applicable to all types of microscopic quantum systems since it works in Hilbert space like in the procedure developed in ref. [14].

In the present work we concentrate on the use of the algorithm in order to characterise and study interacting systems in the vicinity of discontinuous (first order) phase transitions and avoided crossings which are signalized by the existence of fixed points at which coupling constants stay constant during the reduction process. We investigate the ability of the algorithm to perform the reduction of the Hilbert space dimensions at the location of these fixed points and to signalize the existence of phase transition points.

The outline of the paper is the following. In section 2 we recall briefly the main lines of the space reduction algorithm which has been developed elsewhere [9] and show the implication of the existence of fixed points on the

coupling strengths which enter the Hamiltonian of the system. In section 3 we test the algorithm in the neighbourhood of fixed points which correspond to discontinuous transitions and avoided crossings in frustrated spin ladders. Conclusions are drawn in section 4.

2 Formal algorithm and determination of fixed points

2.1 Space reduction procedure.

2.1.1 General concept

We consider a system described by a Hamiltonian $H^{(N)}(g_1^{(N)}, g_2^{(N)}, \dots, g_p^{(N)})$ which depends on p coupling strengths $\{g_1^{(N)}, g_2^{(N)}, \dots, g_p^{(N)} \mapsto g^{(N)}\}$ and acts in a Hilbert space $\mathcal{H}^{(N)}$ of dimension N . $H^{(N)}$ has N eigenvalues $\{\lambda_i(g^{(N)}), i = 1, \dots, N\}$ and eigenvectors $\{|\Psi_i^{(N)}(g^{(N)})\rangle, i = 1, \dots, N\}$.

If the relevant properties of the system are essentially located in a subspace $\mathcal{H}^{(M)}$ of $\mathcal{H}^{(N)}$ ($M < N$) it makes sense to try to define a new effective Hamiltonian $H^{(M)}(g^{(M)})$ whose eigenvalues reproduce the selected subspace and verifies

$$H^{(M)}(g^{(M)})|\Psi_i^{(M)}(g^{(M)})\rangle = \lambda_i(g^{(M)})|\Psi_i^{(M)}(g^{(M)})\rangle$$

with the constraints

$$\lambda_i(g^{(M)}) = \lambda_i(g^{(N)}) \quad (1)$$

for $i = 1, \dots, M$. If this can be realized Eq. (1) implies a relation between the coupling constants in the original and reduced space

$$g_k^{(M)} = f_k(g_1^{(N)}, g_2^{(N)}, \dots, g_p^{(N)})$$

with $k = 1, \dots, p$. We show below how this effective Hamiltonian $H^{(M)}(g^{(M)})$ can be constructed.

2.1.2 Reduction algorithm and renormalization of the coupling strengths.

Consider a system described by a Hamiltonian depending on a unique coupling strength g which can be written as a sum of two terms

$$H = H_0 + H_1(g) \quad (2)$$

The Hilbert space $\mathcal{H}^{(N)}$ of dimension N is spanned by a set of basis states $\{|\Phi_i\rangle, i = 1, \dots, N\}$ which may be chosen as eigenstates of H_0 . An eigenvector $|\Psi_1^{(N)}\rangle$ can be decomposed on this basis

$$|\Psi_1^{(N)}\rangle = \sum_{i=1}^N a_{1i}^{(N)}(g^{(N)})|\Phi_i\rangle \quad (3)$$

Using the Feshbach projection method [15] $\mathcal{H}^{(N)}$ is decomposed into subspaces by means of the projection operators P and Q ,

$$\mathcal{H}^{(N)} = P\mathcal{H}^{(N)} + Q\mathcal{H}^{(N)}$$

Here the subspace $P\mathcal{H}^{(N)}$ is chosen to be of dimension $\dim P\mathcal{H}^{(N)} = N - 1$ by elimination of one basis state. The projected eigenvector $P|\Psi_1^{(N)}\rangle$ obeys the Schroedinger equation

$$H_{eff}(\lambda_1^{(N)})P|\Psi_1^{(N)}\rangle = \lambda_1^{(N)}P|\Psi_1^{(N)}\rangle. \quad (4)$$

where $H_{eff}(\lambda_1^{(N)})$ operates in the subspace $P\mathcal{H}^{(N)}$. It is a nonlinear function of the eigenvalue $\lambda_1^{(N)}$ [9], the eigenenergy being equal to the eigenvalue associated to $|\Psi_1^{(N)}\rangle$ in the initial space $\mathcal{H}^{(N)}$. In practice the coupling $g^{(N)}$ which characterizes the Hamiltonian $H^{(N)}$ in $\mathcal{H}^{(N)}$ is aimed to be changed in such a way that the eigenvalue in the new space $\mathcal{H}^{(N-1)}$ is the same as the one in the complete space $\mathcal{H}^{(N)}$

$$\lambda_1^{(N-1)} = \lambda_1^{(N)}. \quad (5)$$

Hence the reduction of the vector space from N to $N - 1$ results in a renormalization of the coupling constant from $g^{(N)}$ to $g^{(N-1)}$ preserving the physical eigenenergy $\lambda_1^{(N)}$, i.e. $\lambda_1^{(N)} = \lambda_1^{(N-1)} = \lambda_1$. The determination of $g^{(N-1)}$ by means of the constraint expressed by Eq. (5) is the central point

of the procedure. If the dependence on g is linear, i. e. $H = H_0 + gH_1$, it is obtained as a solution of an algebraic equation of the second degree in $g^{(N-1)}$, see Eq.(17) in Ref. [9].

Starting from $\mathcal{H}^{(N-1)}$ the reduction procedure is iterated step by step in decreasing dimensions of the Hilbert space, $N \mapsto N-1 \mapsto N-2 \mapsto \dots$. At each step g is renormalized to a new value. In the limit where the dimensions of \mathcal{H} are very large one may go over to continuous space dimensions, $(n, n-1) \mapsto (x, x-dx)$, and the evolution of g will be given by a flow equation, see Eq.(24) in Ref. [9] and Ref. [16]. The algorithm can be generalized to Hamiltonians depending on several coupling constants.

2.1.3 Remarks.

- The implementation of the reduction procedure asks for the knowledge of λ_1 and the corresponding eigenvector $|\Psi_1^{(k)}\rangle$ at any size k of the vector space. The eigenvalue is in principle fixed as being the physical ground state energy of the system. We use the Lanczos algorithm which allows to determine λ_1 and $|\Psi_1^{(k)}\rangle$ [7, 23, 24]. Consequently this algorithm has been implemented at each step of the reduction process [10].
- The process does not guarantee a rigorous stability of the eigenvalue λ_1 . Indeed one notices that $|\Psi_1^{(k-1)}\rangle$ which is the eigenvector in the space $\mathcal{H}^{(k-1)}$ and the projected state $P|\Psi_1^{(k)}\rangle$ of $|\Psi_1^{(k)}\rangle$ into $\mathcal{H}^{(k-1)}$ may differ from each other. As a consequence it may not be possible to keep $\lambda_1^{(k-1)}$ rigorously equal to $\lambda_1^{(N)} = \lambda_1$. In practice the degree of accuracy depends on the relative size of the eliminated amplitudes $a_{1k}^{(k)}(g^{(k)})$. We shall come back to this point when the algorithm will be implemented in numerical tests.
- The reduction procedure needs a fixed ordering of the sequentially eliminated basis states. This ordering may be chosen by following different criteria. Here the states are arranged according to increasing energies $\epsilon_i = \langle \Phi_i^{(N)} | H | \Phi_i^{(N)} \rangle$ and eliminated starting from the one which corresponds to the highest energy at each step of the procedure.
- The algorithm will be used in applications of the procedure on explicit models, here frustrated spin ladders, and tested in different symmetry

schemes. As already mentioned we concentrate on aspects related to systems close to phase transition points.

2.2 Fixed points

The eigenvalues $\lambda_k(g)$ of $H(g) = H_0 + H_1(g)$ are analytic functions of g which may show algebraic singularities [17, 18, 20] at so called exceptional points $g = g_e$. Exceptional points are first order branch points in the complex g - plane which appear when two (or more) eigenvalues get degenerate. This can happen if g takes values such that $\epsilon_k = \epsilon_l$ where $\epsilon_k = \langle \Phi_k | H | \Phi_k \rangle$. In a finite Hilbert space the degeneracy appears as an avoided crossing for real g . If an energy level ϵ_k belonging to the $P\mathcal{H}$ subspace defined above crosses an energy level ϵ_l lying in the complementary $Q\mathcal{H}$ subspace the perturbation development constructed from $H_{eff}(E)$ diverges [20].

Due to symmetry properties physical states can get degenerate in energy for real values of g_e . They correspond to first order phase transitions.

Exceptional points are defined as the solutions of [18, 20]

$$f(\lambda(g_e)) = \det[H(g_e) - \lambda(g_e)I] = 0 \quad (6)$$

and

$$\left. \frac{df(\lambda(g_e))}{d\lambda} \right|_{\lambda=\lambda(g_e)} = 0 \quad (7)$$

It is possible to show that exceptional points are fixed points of the coupling strength g which stay constant during the space reduction process.

If $\{\lambda_i(g)\}$ are the set of eigenvalues the secular equation can be written as

$$\prod_{i=1}^N (\lambda - \lambda_i) = 0 . \quad (8)$$

Consider $\lambda = \lambda_p$ which satisfies Eq. (6). Eq. (7) can only be satisfied if there exists another eigenvalue $\lambda_q = \lambda_p$, hence if a degeneracy appears in the spectrum. This is the case at an exceptional point.

If the eigenvalue $\lambda_j^{(k)}$, $k = N, N-1, \dots$ which is either constant or constrained to take the fixed value λ_j gets degenerate with some other eigenvalue $\lambda_i^{(k)}(g = g_e)$ in the space reduction process this eigenvalue must obey

$$\lambda_i^{(k)}(g_e) = \lambda_i^{(l)}(g'_e) \quad (9)$$

which is realised in any projected subspace of size k and l containing states $|\Phi_j\rangle$ and $|\Phi_i\rangle$. Going over to the continuum limit for large values of N as introduced above and considering the subspaces of dimension x and $x + dx$

$$\lambda_i(g_e(x), x) = \langle \Psi_i(g_e(x), x) | H(g_e(x)) | \Psi_i(g_e(x), x) \rangle$$

verifies

$$\frac{d\lambda_j}{dx} = 0 = \frac{d\lambda_i(g_e(x), x)}{dx} \quad (10)$$

Consequently

$$\frac{\partial \lambda_i}{\partial x} + \frac{\partial \lambda_i}{\partial g_e} \frac{dg_e}{dx} = 0 \quad (11)$$

Since $\lambda_i(g_e(x), x)$ does not move with x in the space dimension interval $(x, x + dx)$ the first term in Eq. (11) is equal to zero. Hence in general

$$\frac{\partial \lambda_i}{\partial g_e} \neq 0 \quad \text{and} \quad \frac{dg_e}{dx} = 0 \quad (12)$$

The present result is general, it is valid for both continuous and discontinuous quantum phase transitions. Avoided crossings reflect the existence of continuous transitions in the limit of systems of infinite size. In the case of discontinuous (first order) transitions the energies of the physical states $\{|\Psi_i\rangle\}$ show a real degeneracy point, i.e. their energies cross at real values of $g = g_e$ as already mentioned above.

In the following we shall consider Hamiltonians linear in g , $H(g) = H_0 + gH_1$. A sufficient condition for possible level crossings is given by

$$[H_0, H_1] = 0 \quad (13)$$

i.e. H_0 and H_1 can be simultaneously diagonalized [8, 19]. In this case if H_0 is diagonal in the $\{|\Phi_i\rangle, i = 1, \dots, N\}$ basis of states it is also an eigenbasis for H and

$$\frac{d\lambda_i(g_e(x), x)}{dx} = \frac{d\langle \Phi_i | H_0 + g_e(x)H_1 | \Phi_i \rangle}{dx} \quad (14)$$

Since H_0 and H_1 do not depend on x , $d\lambda_i/dx = 0$ implies $dg_e/dx = 0$ for this specific form of the Hamiltonian which is consistent with the general result Eq. (12).

2.3 Remarks.

- In the general case $H(g) = H_0 + H_1(g)$ $g(x) = g_e$ evolves through a flow equation which is more complicated than Eq. (24) in [9]. We shall restrict our numerical investigations to Hamiltonians which show a linear dependence on g .
- The energy level crossings can occur for any two energy eigenstates of the spectrum. We shall consider level crossings or avoided crossings between the ground state and an excited state as well as the case of crossings or avoided crossings of excited states.

The present formal considerations are now used in numerical applications. We analyze the behaviour of the reduction algorithm in the neighbourhood of fixed points and show to what extent it allows to detect fixed points in an application to two-legged frustrated spin ladders for different choices of the basis of states.

3 Application to quantum transitions in frustrated two-leg quantum spin ladders.

3.1 The model

3.1.1 SU(2)-symmetry framework.

Consider spin-1/2 ladders [21, 22] shown in Fig. 1 and described by Hamiltonians of the following type

$$\begin{aligned}
H^{(s,s)} = & J_t \sum_{i=1}^L s_{i1} s_{i2} + J_l \sum_{\langle ij \rangle} s_{i1} s_{j1} + J_l \sum_{\langle ij \rangle} s_{i2} s_{j2} \\
& + J_{1c} \sum_{(ij)} s_{i1} s_{j2} + J_{2c} \sum_{(ij)} s_{i2} s_{j1}
\end{aligned} \tag{15}$$

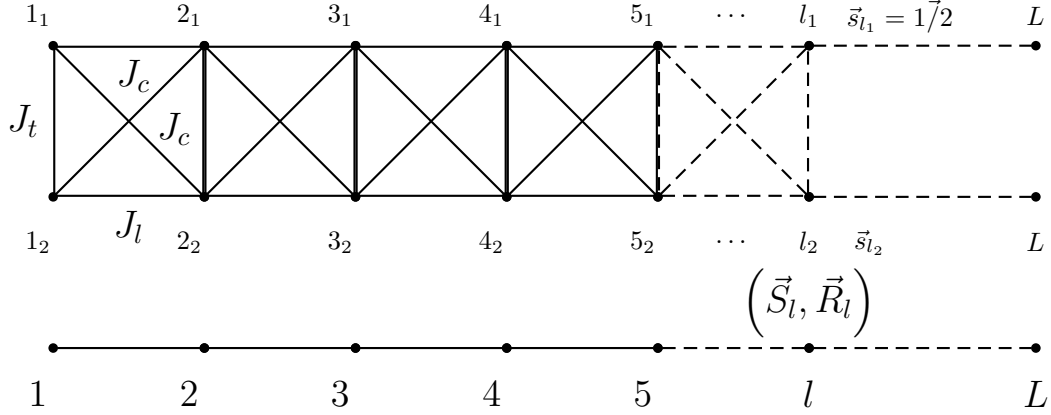


Figure 1: Top: the original spin ladder. The coupling strengths are indicated as given in the text. Bottom: The ladder in the SO(4) representation. See the text.

Working in a representation with fixed total magnetic projection M_{tot} the basis of states is spanned by the vectors $\{|\Phi_k\rangle, k = 1, \dots, N\}$ where

$$|\Phi_k\rangle = |1/2 \ m_1, \dots, 1/2 \ m_i, \dots, 1/2 \ m_{2L}, \sum_{i=1}^{2L} m_i = M_{tot}\rangle$$

and $\{m_i = +1/2, -1/2\}$.

The indices 1 or 2 label the spin $1/2$ vector operators s_{i_k} acting on the sites i on both ends of a rung, in the second and third term i and j label nearest neighbours, here $j = i + 1$ along the legs of the ladder. The fourth and fifth term correspond to diagonal interactions between nearest sites located on different legs. $2L$ is the number of sites on a ladder. Here we fix $J_{1c} = J_{2c} = J_c$. The coupling strengths J_t, J_l, J_c are positive. In the sequel we restrict our analysis to the case where $M_{tot} = 0$.

In the present applications the renormalization is restricted to a unique coupling strength, see Eq. (2). It is implemented here by putting $H_0 = 0$

and $H^{(N)} = g^{(N)} H_1$ where $g^{(N)} = J_t$ and

$$\begin{aligned}
H_1 = & \sum_{i=1}^L s_{i1} s_{i2} + \gamma_{tl} \sum_{\langle ij \rangle} (s_{i1} s_{j1} + s_{i2} s_{j2}) \\
& + \gamma_c \sum_{\langle ij \rangle} (s_{i1} s_{j2} + s_{i2} s_{j1})
\end{aligned} \tag{16}$$

where $\gamma_{tl} = J_l/J_t$, $\gamma_c = J_c/J_t$. These quantities are kept fixed and $g^{(N)} = J_t$ will be subject to renormalization in the reduction process.

3.1.2 $SO(4)$ -symmetry framework.

The basis of states may be written in an $SO(4)$ -symmetry scheme. By means of a spin rotation [25, 26]

$$s_{i1} = \frac{1}{2}(S_i + R_i) . \tag{17}$$

$$s_{i2} = \frac{1}{2}(S_i - R_i) . \tag{18}$$

the Hamiltonian Eq.(15) can be expressed in the form

$$\begin{aligned}
H^{(S,R)} = & \frac{J_t}{4} \sum_{i=1}^L (S_i^2 - R_i^2) + J_1 \sum_{\langle ij \rangle} S_i S_j \\
& + J_2 \sum_{\langle ij \rangle} R_i R_j
\end{aligned} \tag{19}$$

which reduces the ladder formally to a chain, see bottom of Fig. 1. Here $J_1 = (J_l + J_c)/2$, $J_2 = (J_l - J_c)/2$, $J_{1c} = J_{2c} = J_c$. The components $S_i^{(+)}, S_i^{(-)}, S_i^{(z)}$ and $R_i^{(+)}, R_i^{(-)}, R_i^{(z)}$ of the vector operators S_i and R_i are the $SO(4)$ group generators and $\langle ij \rangle$ denotes nearest neighbour rung indices

$$S_i^{(+)} = \sqrt{2}(X_i^{(11)(10)} + X_i^{(10)(1-1)}) = S_i^{(-)*}$$

$$S_i^{(z)} = X_i^{(11)(11)} - X_i^{(1-1)(1-1)}$$

$$R_i^{(+)} = \sqrt{2}(X_i^{(11)(00)} - X_i^{(00)(1-1)}) = R_i^{(-)*}$$

$$R_i^{(z)} = -(X_i^{(10)(00)} + X_i^{(00)(10)})$$

where

$$X_i^{(S_i M_i)(S'_i M'_i)} = |S_i M_i\rangle \langle S'_i M'_i|$$

with states defined as

$$|S_i M_i\rangle = \sum_{m_1, m_2} \langle 1/2 \ m_1 \ 1/2 \ m_2 | S_i M_i \rangle |1/2 \ m_1\rangle_i |1/2 \ m_2\rangle_i$$

along a rung are coupled to $S_i = 0$ or $S_i = 1$. Spectra are constructed in this representation as well as in the $SU(2)$ representation.

In a representation with fixed total magnetic projection $M_{tot} = 0$ the basis of states is then spanned by the vectors

$$|\Phi_k\rangle = |S_1 M_1, \dots, S_i M_i, \dots, S_L M_L, \sum_{i=1}^L M_i = M_{tot} = 0\rangle$$

and $\{M_i = 0, +1, -1\}$

In the sequel we analyse the behaviour of the system in both symmetry frames.

3.2 Fixed points in the $SU(2)$ -symmetry framework.

3.2.1 First order phase transitions of the two-legged spin ladder.

At first order transitions which happen at level crossings for real g the amplitudes of the wavefunctions are expected to acquire weights of the same order of magnitude over a large number of basis states. The analyses performed

in [10] show that the use of the algorithm at fixed points should work as a stringent test of the method.

The first application concerns a system described by the Hamiltonian $H^{(s,s)}$ given by Eq. (15) using an $SU(2)$ -symmetry basis of states given below Eq. (15). A crossing between a rung dimer phase and a Haldane phase appears for $J_t = J_c$ when $J_t/J_l \simeq 1.401$ in the case of an asymptotically large system [21, 22, 28, 29, 30, 31]. The ratio depends on the size of the system. The existence of a first order transition is analysed below, the coupling constant $g = J_t$ is expected to stay constant at the level crossing point.

3.2.2 Application of the reduction algorithm at fixed points.

We consider ladders with $L = 6$. Several crossings between energy levels can be observed in Fig. 2(a) which shows the evolution of the energies of the four lowest states in the $M_{tot} = 0$ subspace as a function of $g = J_t$. The crossing between the ground state energy e_1 and the energy of the first excited state e_2 corresponds to $J_t/J_l \simeq 1.23$.

The first test corresponds to $J_t \geq 6$. Then the three lowest excited states corresponding to e_2, e_3, e_4 get rigorously degenerate which generates a continuous transition line [29]. Fixing $J_t = 10$ Fig. 2(b) shows the evolution of the four lowest states as a function of the size N of the Hilbert space following the algorithm described in Refs. [9, 10]. The initial space dimension is $N = 924$. The stability of the spectrum is remarkable down to $N \leq 100$. This stability reflects in the constancy of J_t over the same dimensional range, see Fig. 2(c). For lower values of N deviations appear. They are due to the approximations inherent to the projection method as noted in the second remark of subsection 2.1.3 and Refs. [9, 10]. The limit of constancy of J_t indicates the minimum dimension of Hilbert space in which diagonalization will lead to the reproduction of the low energy part of the spectrum, i. e. the ground and first excited states. The behaviour of the spectrum shown here is observed for any value of $J_t \geq 6$, i. e. all along the degeneracy lines.

Fig. 2(d) gives the evolution of the entropy s per site defined as [32]

$$s = -\frac{1}{2L} \sum_{i=1}^N P_i \ln P_i \quad \text{with} \quad P_i = |\langle \Phi_i^{(N)} | \Psi_1^{(N)} \rangle|^2 = |a_{1i}^{(N)}|^2 \quad (20)$$

at the fixed point $J_t = 5$ which corresponds in Fig. 2(a) to the crossing of the ground state e_1 with the first excited state e_2 . Here $\{a_{1i}^{(N)}\}$ are the

amplitudes of the components of the ground state wavefunction developed on the basis of states $\{|\Phi_i >\}$ which span the space of dimension N . The step discontinuity signals the transition characterized by a strong change in the structure of the lowest state. The characteristic singularity observed at this value of J_t is conserved as long as the ground state keeps stable during the space reduction process.

At the exact location of the fixed point the instability of the spectrum is sizable and the coupling constant J_t at this crossing point stays constant over a smaller interval of values of N . A closer inspection shows that this instability might be related to a numerical difficulty in the renormalization of J_t . Indeed the coefficients of the algebraic second order equation which fixes it [9] get accidentally vanishingly small at this place and consequently lead to strongly unprecise values of the roots of the equation. This corresponds to a pathological situation which may not be significative in the general case. Indeed, in the close neighbourhood of the fixed point, J_t stays stable over a much larger interval of values of N when $J_c = 3.8 \neq J_l$ (see Figs. 2 (e) and 2(f)).

3.3 Fixed points in the $SO(4)$ -symmetry framework - First order transitions

The reduction algorithm is next applied to the same system as above but described by the Hamiltonian $H^{(S,R)}$ given by Eq. (19) with a basis of states $\{|\Phi_i >\}$ written in the $SO(4)$ symmetry framework introduced in subsection 3.1.2. The spectrum given in Fig. 3(a) in the $M_{tot} = 0$ subspace is the same as in the case of the $SU(2)$ symmetry framework as it should be. However the behaviour of the numerically generated spectrum at different transition points is quite different.

At the crossing point between the ground state and the first excited state in the $M_{tot} = 0$ subspace which occurs at $J_t = 5$ (see Fig. 3(a)) the ground state energy e_1 and J_t remain stable all along the space dimension reduction procedure as seen in Figs. 3(b) and 3(c). This remarkable stability can be explained by the fact that the ground state wavefunction is strongly dominated by a small number of states in the $SO(4)$ basis. It is however lost for the first excited state with energy e_2 which moves abruptly and stays then again constant generating successive plateaus over more or less large intervals in N , Fig. 3(b). This shows that $d\lambda_i/dx = 0$, ($i = 2, 3, 4$) is indeed preserved

by steps, but not necessarily λ_i which jumps by steps over finite intervals of space dimensions. The jumps in $\{\lambda_i\}$ may be related to the elimination of non negligible components of the wavefunction during the reduction process.

Fig. 3(d) shows the behaviour of s the ground state entropy per site which behaves like in the $SU(2)$ scheme but is quantitatively smaller. This is due to the fact that the wavefunction amplitudes are less equally distributed here than in the $SU(2)$ -scheme as mentioned above. Figs. 3(e) and 3(f) show the behaviour of the spectrum and coupling constant J_t in the close neighbourhood of the transition point. One observes that the evolution of the energies is smoother than at the transition point itself and the coupling constant increases slightly with decreasing N . Some curves in the figures are drawn with a finite width in order to facilitate the observation of the stepwise evolution of the corresponding quantities. Degeneracy of the states and the consequent constancy for $J_t \geq 6$ is observed along $e_2 = e_3 = e_4$ which corresponds to a transition line as seen in Figs. 4(a) and 4(b). The constancy of these quantities is preserved over the whole range of space dimensions N , except for $\{e_i\}$'s at small N . But $\{e_i\}$'s stay more and more constant up to the smallest values of N with increasing J_t , see Figs. 4(c) and 4(d). This can be explained by the fact that the wavefunctions gets more and more dominated by a small number of basis states with increasing J_t . Evidently the robustness of the spectrum is stronger in the present symmetry scheme than in the case of $SU(2)$.

3.4 Application of the reduction algorithm at a continuous transition: avoided crossings.

As already mentioned continuous transitions reduce to avoided crossings in finite systems. States get degenerate at complex values of this parameter. Genuine transitions with real parameters cannot be explicitly seen in numerically determined spectra of finite systems. Avoided crossings are not easy to locate. They occur at complex exceptional points and the present numerical procedure is aimed to follow the evolution of real running coupling constants.

Fig. 5(a) shows the spectrum of the ladder for specific values of the coupling constants. One observes several possible avoided crossings which are rather close to each other in the interval $4 < J_t < 9$. The typical behaviour of the spectrum is shown in Fig. 5(b) for $J_t = 6.6891$. Fig. 5(c) gives a

quantitative estimate of the energy fluctuations of excited states. Here

$$p(i) = \left| \frac{e_i^{(N)} - e_i^{(N-k)}}{e_i^{(N)}} \right| \times 100 \quad \text{with } i = 1, \dots, 4$$

The spectrum and J_t are relatively stable down to $N \simeq 200$. Stability is lost below this value. The same is true at other avoided crossing points. These points are difficult to locate, the coupling J_t is complex there and our procedure does not fix their imaginary part. It may be that clearer signals can be observed for larger systems since then the gap at crossings gets smaller (in principle tends to zero in case of a continuous transition) and hence leads to a reduced the imaginary part of the coupling constant.

Remarks:

- In the present calculations the system has open boundary conditions. For odd L the entropy shows the same characteristic discontinuity as observed for first order transitions in Figs. 2(d) and 3(d) at the transition point. For L even the discontinuity goes over in a finite peak which recalls a continuous transition in a finite size system. This shows that a naive interpretation of observables in finite systems can lead to erroneous interpretations of the order of a transition.
- Expected crossings may not necessarily signal continuous transitions in the limit of infinite systems. In this limit the order may effectively be different. This phenomenon has also been observed in classical systems see f.i. [33] and references therein.

4 Summary, conclusions and outlook.

We used an algorithm which aims to reduce the size of the Hilbert space of states describing strongly interacting systems. The reduction induces a renormalization of coupling constants which enter the Hamiltonians of the systems, here frustrated two-leg quantum spin ladders. The robustness of the algorithm has already been tested in former work [10].

We applied the algorithm at the location and in the neighbourhood of first order transition points and lines, and in the vicinity of avoided crossings which correspond to second order transitions in infinite systems. The

analysis has been pursued in two different symmetry schemes. As it may be expected the behaviour of the spectrum and the renormalized coupling parameter depend on the symmetry framework. Indeed, the description of the system depends crucially on the details of the wavefunctions of the different energy states and their structure is different in different representations.

In the case of first order transitions we showed that the renormalized coupling constant J_t may indeed be numerically stable over a large set of dimensions of Hilbert space and signal the presence of a transition as predicted by the theory considerations developed in section 2.2. Strong instabilities may appear due to accidental numerical pathologies as mentioned in section 3.2.2.

The stability is larger in the case of an $SO(4)$ -symmetry representation where the number of large components is reduced. In the present parameter space the low-lying eigenstates are strongly dominated by a small set of $SO(4)$ basis states. This may also explain the stronger stability of degenerate states at the crossing points and along transition lines.

Avoided crossings have also been investigated. The presence of these points is difficult to locate. It may be due to the fact that the level crossing point occurs for a complex coupling constant which is not detected in the present algorithm. The precise understanding of these points related to numerics requires further work which lies outside the scope of the present investigations.

It may be mentioned here that there exists other methods which are aimed to detect crossing and avoided crossing points. One of them relies on discontinuities in the entanglement properties of wavefunctions [34, 35] which have to be known at crossing (first order transitions) or avoided crossings (continuous transitions). A second approach relies on an algebraic method [36] which works very nicely in the case of small systems. It is not clear however whether its use can be easily applied to very large Hilbert spaces such as those which correspond to realistic quantum spin systems.

In summary, the present investigations show that first order transition points in quantum spin systems may be correlated with strong fluctuations in the energies of low-lying excited states. The presence of these points are signalized by the constancy of the strength of the couplings which enter the Hamiltonian along the dimensional reduction procedure of Hilbert space. This is predicted by theoretical considerations and verified, at least up to the point at which numerical stability gets lost which may happen at different stages of the reduction procedure depending on the structure of the ground state wavefunction.

One of us (T.K.) would like to thank Drs. T. Vekua and R. Santachiara for critical remarks and helpful advice.

References

- [1] K. G. Wilson, Phys. Rev. Lett. **28** (1972) 548; Rev. Mod. Phys. **47** (1975) 773
- [2] Jean-Paul Malrieu and Nathalie Guithéry, Phys.Rev. **B63** (1998) 085110
- [3] S. Capponi, A. Lauchli, M. Mambrini, Phys.Rev. **B70** (2004) 104424
- [4] S. R. White and R. M. Noack, Phys. Rev. Lett. **68** (1992) 3487
- [5] A. L. Malvezzi, cond-mat/0304375, Braz. J. Phys. **33** (2003) pages 55 - 72
- [6] S. R. White, Phys. Rev. Lett. **69** (1992) 2863
- [7] M. Henkel, “Conformal invariance and critical phenomena”, Springer Verlag, 1999
- [8] S. Sachdev, ”Quantum Phase Transitions”, Cambridge University Press, 1999
- [9] T. Khalil and J. Richert, J. Phys. A: Math. Gen. **37** (2004) 4851-4860
- [10] T. Khalil and J. Richert, quant-ph/0606056
- [11] S. D. Glazek and Kenneth G. Wilson, Phys. Rev. **D57** (1998) 3558
- [12] H. Mueller, J. Piekarewicz and J. R. Shepard, Phys. Rev. **C66** (2002) 024324
- [13] K. W. Becker, A. Huebsch and T. Sommer, Phys.Rev. **B66** (2002) 235115
- [14] Roi Baer and Martin Head-Gordon, Phys.Rev. **B58** (1998) 15296
- [15] H. Feshbach, Nuclear Spectroscopy, part B, Academic Press (1960)
- [16] J. Richert, quant-ph/0209119

- [17] T. Kato, "Perturbation Theory for Linear Operators", Springer Verlag, Berlin, 1966
- [18] W. D. Heiss, Phys. Rev. **E61** (2000) 929
- [19] W. D. Heiss, Eur. Phys. J. **D7** (1999) 1
- [20] T. H. Schucan and H. A. Weidenmüller, Ann. Phys. (N.Y.) **76** (1973) 483
- [21] H. Q. Lin and J. L. Shen, J. Phys. Soc. Japan, **69** (2000) 878
- [22] H. Q. Lin, J. L. Shen and H. Y. Schick, Phys.Rev. **B66** (2002) 184402
- [23] N. Laflorencie and D. Poilblanc, Lect. Notes Phys., vol. 645, pages 227 - 252 (2004)
- [24] Jane K. Cullum and Ralph A. Willoughby, Lanczos Algorithms for Large Symmetric Eigenvalue Computations, vol. I: Throry, Classics in Applied Mathematics, siam 1985
- [25] K. Kikoin, Y. Avishai and M. N. Kiselev, in "Molecular nanowires and Other Quantum Objects", A. S. Alexandrov and R. S. Williams eds., NATO Sci. Series II, vol. 148, p. 177 - 189 (2004), cond-mat/0309606
- [26] M. N. Kiselev, K. Kikoin and L. W. Molenkamp, Phys.Rev. **B68** (2003) 155323
- [27] J. Richert, cond-mat/0510343
- [28] Martin P. Gelfand, Phys.Rev. **B43** (1991) 8644
- [29] Zheng Weihong, V. Kotov and J. Oitmaa, Phys.Rev. **B57** (1998) 11439
- [30] Indrani Bose, cond-mat/0208039
- [31] Xiaoqun Wang, Mod. Phys. Lett. **B14** (2000) 327, cond-mat/9803290.
- [32] Valentin V. Sokolov, B. Alex Brown and Vladimir Zelevinsky, Phys. Rev **E58** (1998) 56
- [33] M. Pleimling and A. Hueller, J. Stat. Phys. **104** (2006) 140405

- [34] L.-A. Wu, M. S. Sarandy and D. A. Lindar, Phys. Rev. Lett. **93** (2004) 250404
- [35] Thiago R. de Oliveira, Gustavo Rigolin, Marcos C. de Oliveira and Eduardo Miranda, Phys. Rev. Lett. **97** (2006) 170401
- [36] M. Bhattacharya and C. Raman, Phys. Rev. Lett. **97** (2006) 140405

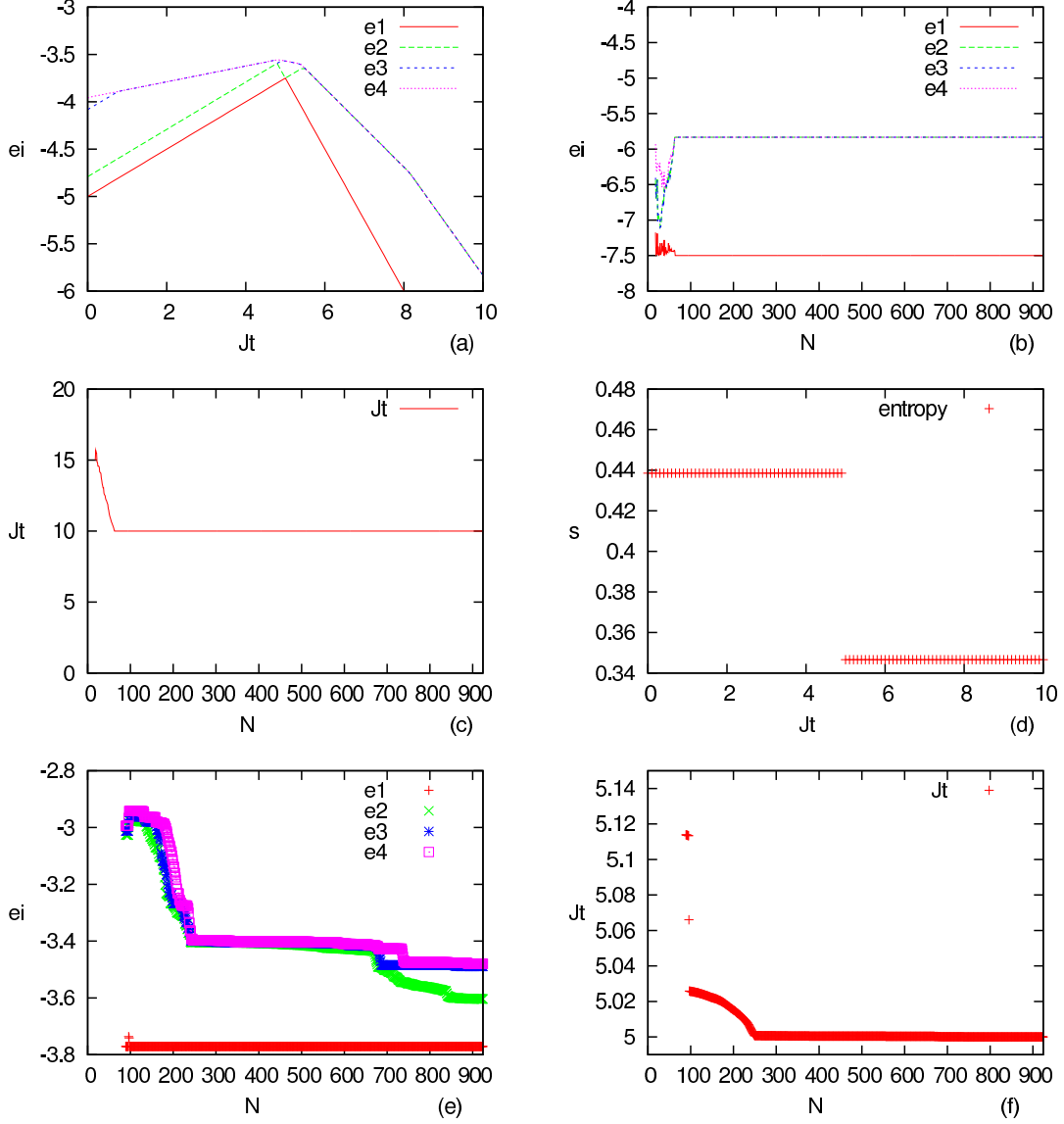


Figure 2: $SU(2)$ -symmetry scheme. The $\{e_i, i = 1, 2, 3, 4\}$ are the energies per site of the ground and lowest excited states. N is the size of the Hilbert space, s the entropy of the ground state per site. The number of sites is $L = 6$ along a leg, $J_l = J_c \simeq 4.07$. (b) and (c) correspond to $J_t = 10$. Figs.(e) and (f) correspond to $J_c = 3.8 \neq J_l$. Broadened lines are drawn for the sake of readability. See discussion in the text.

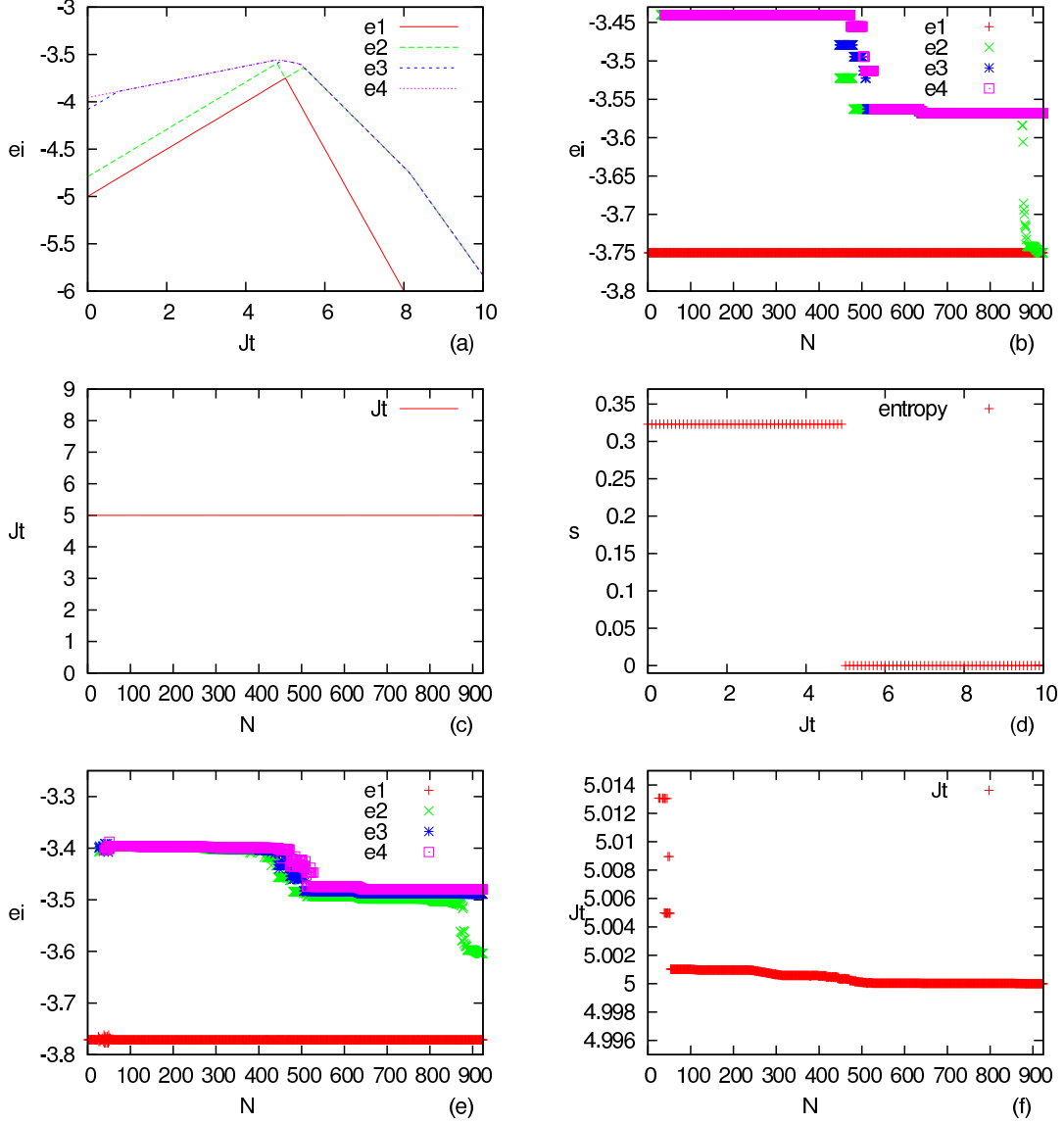


Figure 3: $SO(4)$ -symmetry scheme. The $\{e_i, i = 1, 2, 3, 4\}$ are the energies per site of the ground and lowest excited states. N is the size of the Hilbert space, s the entropy of the ground state per site. The number of sites is $L = 6$ along the chain. (a) - (d): $J_l = J_c$. In (b) and (c) $J_t = 5$ (e) - (f): $J_t = 5$, $J_l \neq J_c$, $J_c = 3.8$. In both cases $J_t/J_l \simeq 1.23$. Broadened lines are drawn for the sake of readability. See discussion in the text.

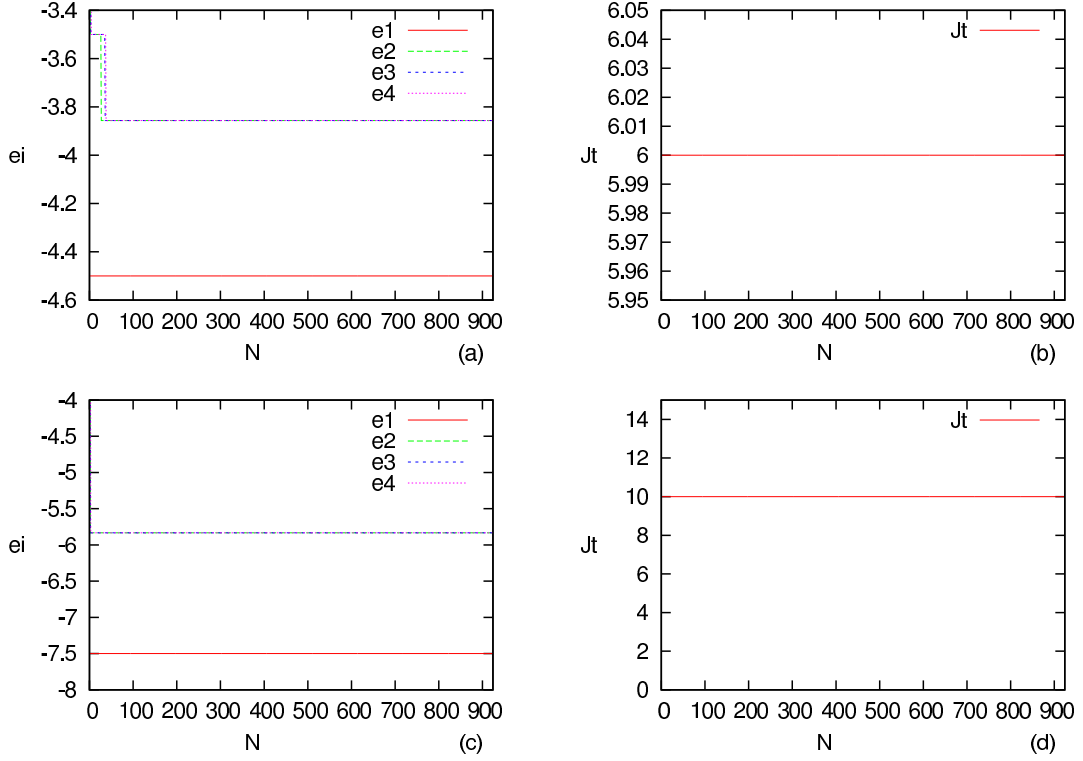


Figure 4: $SO(4)$ -symmetry scheme. The $\{e_i, i = 1, 2, 3, 4\}$ are the energies of the ground and lowest excited states per site. The number of sites is $L = 6$ along the chain, $J_l = J_c \simeq 4.07$. (a) and (b) correspond to $J_t = 6$, (c) and (d) correspond to $J_t = 10$. See discussion in the text.

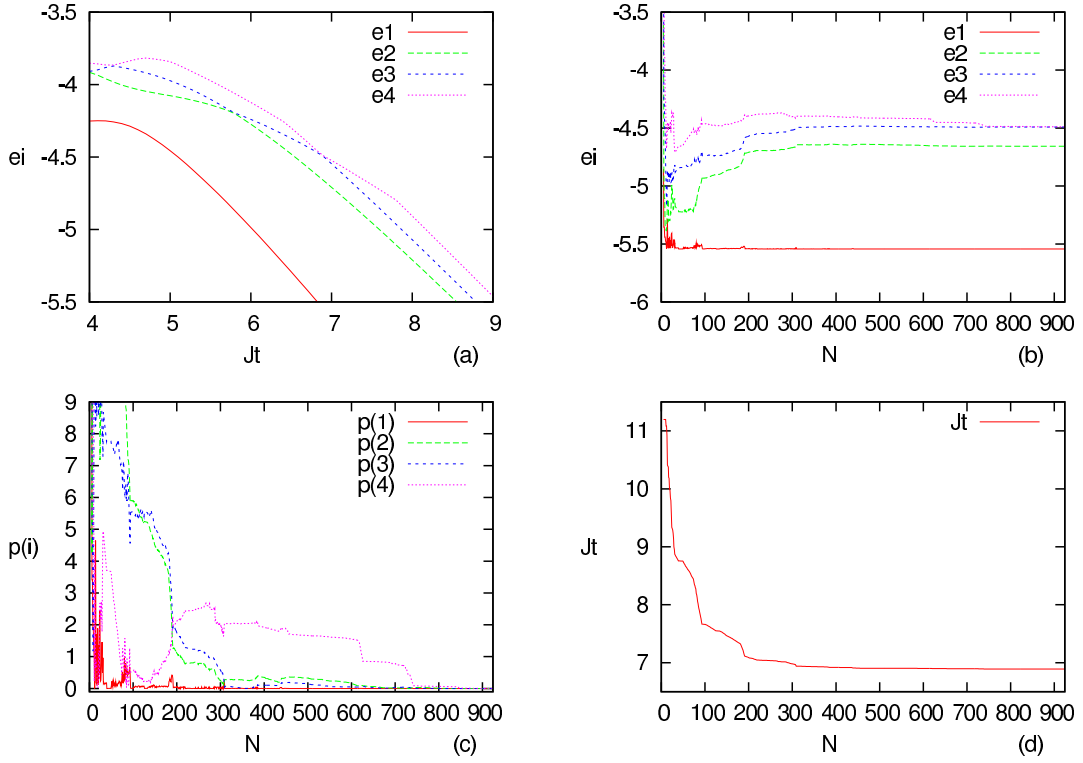


Figure 5: $SU(2)$ -symmetry scheme. The $\{e_i, i = 1, 2, 3, 4\}$ are the energies per site of the ground and excited states. N is the size of the Hilbert space. The number of sites is $L = 6$ sites, $J_t = 6.891$, $J_l = 5$, $J_c = 3$. See discussion in the text